Cooperative Concurrent Mapping and Localization

John W. Fenwick, Paul M. Newman, and John J. Leonard
Massachusetts Institute of Technology
77 Mass Ave., Cambridge, MA 02139

fenwickjw@hotmail.com,pnewman@mit.edu,jleonard@mit.edu

Abstract—Autonomous vehicles require the ability to build maps of an unknown environment while concurrently using these maps for navigation. Current algorithms for this concurrent mapping and localization (CML) problem have been implemented for single vehicles, but do not account for extra positional information available when multiple vehicles operate simultaneously. Multiple vehicles have the potential to map an environment more quickly and robustly than a single vehicle. This paper presents a cooperative CML algorithm that merges sensor and navigation information from multiple autonomous vehicles. The algorithm presented is based on stochastic estimation and uses a feature-based approach to extract landmarks from the environment. The theoretical framework for the collaborative CML algorithm is presented, and a convergence theorem central to the cooperative CML problem is proved for the first time. This theorem quantifies the performance gains of collaboration, allowing for determination of the number of cooperating vehicles required to accomplish a task. A simulated implementation of the collaborative CML algorithm demonstrates substantial performance improvement over non-cooperative CML.

I. INTRODUCTION

Successful operation of an autonomous vehicle requires the ability to navigate. Navigation information consists of positional estimates and an understanding of the surrounding environment. Without this information, even the simplest of autonomous tasks are impossible. An important subfield within mobile robotics that requires accurate navigation is the performance of collaborative tasks by multiple vehicles. Multiple vehicles can frequently perform tasks more quickly and robustly than a single vehicle [1], [2]. However, accomplishing collaborative tasks demands that each vehicle be aware of relative locations of collaborators in addition to the baseline environmental knowledge. This paper considers the problem of performing concurrent mapping and localization (CML) with a team of cooperating autonomous vehicles.

There is a large literature in the use of multiple vehicle robotic systems [3]. Since CML is the union of navigation and mapping, much relevant existing work is found in the separate subfields of collaborative localization and collaborative mapping.

Collaborative navigation is performed when multiple vehicles share navigation and sensor information in order to improve their own position estimate beyond what is possible with a single vehicle. Ant-inspired trail-laying behaviors have been used by a team of mobile robots tasked to navigate towards a common goal [4]. Simple collective navigation has been demonstrated in simulation using multiple 'cartographer' robots that randomly explore the environment [5]. Sty [6] performs simple relative localization between collaborators using directional beacons. Vision-based cooperative localization has been performed by a team of vehicles tasked with cooperatively trapping and moving objects [7]. Tracking via vision is also used for relative localization of collaborators in an autonomous mobile cleaning system [8]. In work by Roumeliotis *et al.* [9], [10], collaborative localization is performed using a distributed stochastic estimation algorithm. Cooperative navigation of autonomous underwater vehicles has been performed in work by Singh *et al.* [11]. Also, two AUVs have demonstrated collaborative operation using the same acoustic beacon array [12]. An unmanned helicopter has used a vision sensor to detect collaborating ground vehicles at globally known positions, and thus was able to localize itself [13].

Collaborative mapping combines sensor information from multiple vehicles to construct a larger, more accurate map. Cooperative mapping and exploration with multiple robots is reported by Mataric [14] using behavior-based control [15]. Map matching is used to combine topological maps constructed by multiple vehicles in work performed by Dedeoglu and Sukhatme [16]. Heterogeneous collaborative mapping has also been investigated, as such systems can capitalize on specialization [17].

In the area of navigation and mapping by multiple vehicles, the work of Thrun and colleagues stands out at the forefront of the current state-of-the-art [18], [19]. Sequential Monte Carlo methods [20] (also known as particle filters) for both multi-robot global localization [19] and real-time CML using SICK laser scanner data. Our work uses a feature-based representation [21], [22], [23]. Another possibility is to use a topological representation [24], [25].

This paper reports the execution of the logical next step in the development of CML: a CML algorithm for use by multiple collaborating autonomous vehicles. Sharing and combining observations of environmental features as well as of the collaborating vehicles can greatly enhance the performance of CML. This pa-

per demonstrates the feasibility and benefits of collaborative CML. Multiple vehicles performing CML together can achieve faster and more thorough mapping, and produce improved relative (and global) position estimates. This paper quantifes the improvement in CML performance achieved by collaboration, and compares collaborative versus single-vehicle CML results in simulation to demonstrate how collaborative CML greatly increases the navigation capabilities of autonomous vehicles.

II. REVIEW OF SINGLE VEHICLE CML

This section reviews stochastic mapping (SM), first introduced by Smith, Self and Cheeseman [26], which provides a theoretical foundation of feature-based CML. The stochastic mapping approach assumes that distinctive stationary features in the environment can be reliably extracted from sensor data, and capitalizes on reobservation of these features to concurrently localize the vehicle and improve feature estimates. SM considers CML as a variable-dimension state estimation problem, where the state size increases or decreases as features are added to or removed from the map. Assuming n static features in the environment, the world state at time k is denoted by a single state vector $\mathbf{x}[k] = [\mathbf{x}_v[k]^T \ \mathbf{x}_f[k]^T]^T$, where $\mathbf{x}_v[k]$ represents the location of the vehicle, and $\mathbf{x}_f[k] = [\mathbf{x}_{f_1}[k]^T \dots \mathbf{x}_{f_n}[k]^T]^T$ represent the locations of the environmental features.

Associated with the state estimate $\mathbf{x}[k]$ is an estimated covariance matrix $\mathbf{P}[k]$, which has the expanded form

$$\mathbf{P}[k] = \begin{bmatrix} \mathbf{P_{vv}}[k] & \mathbf{P_{v1}}[k] & \mathbf{P_{v2}}[k] & \dots & \mathbf{P_{vn}}[k] \\ \mathbf{P_{1v}}[k] & \mathbf{P_{11}}[k] & \mathbf{P_{12}}[k] & \dots & \mathbf{P_{1n}}[k] \\ \mathbf{P_{2v}}[k] & \mathbf{P_{21}}[k] & \mathbf{P_{22}}[k] & \dots & \mathbf{P_{2n}}[k] \\ \vdots & \vdots & \vdots & \ddots & \vdots \\ \mathbf{P_{nv}}[k] & \mathbf{P_{n1}}[k] & \mathbf{P_{n2}}[k] & \dots & \mathbf{P_{nn}}[k] \end{bmatrix}. \quad (1)$$

This equation contains the vehicle ($\mathbf{P_{vv}}[k]$) and feature ($\mathbf{P_{ii}}[k]$) covariances located on the main diagonal. Also contained are the vehicle-feature ($\mathbf{P_{vi}}[k]$) and feature-feature ($\mathbf{P_{ij}}[k]$) cross correlations, located on the off-diagonals.

Given sensor data, the state estimate and associated covariance matrix are updated using an Extended Kalman Filter (EKF). For a complete listing of the equations for the single vehicle SM prediction and update steps, see [27], [28].

III. SINGLE VEHICLE CML PERFORMANCE CHARACTERISTICS

This section briefy reviews theorems from work by Newman and Dissanayake [29][30] that characterize the performance of the single vehicle CML algorithm,

and will be extended to the multiple vehicle case in Section V.

Theorem III.1: The determinant of any submatrix of the map covariance matrix $\mathbf{P}$ decreases monotonically as successive observations are made.

The determinant of a state covariance submatrix is an important measure of the overall uncertainty of the state estimate, as it is directly proportional to the volume of the error ellipse for the vehicle or feature. Theorem III.1 states that the error for any vehicle or feature estimate will never increase during the update step of SM. This makes sense in the context of the structure of SM, as error is added during the prediction step and subtracted via sensor observations during the update step.

Theorem III.2: In the limit as the number of observations increases, the errors in estimated vehicle and feature locations become fully correlated.

Not only do individual vehicle and feature errors decrease as more observations are made, they become fully correlated and features with the same structure (i.e. point features) acquire identical errors. Intuitively, this means that the relative positions of the vehicle and features can be known exactly. The practical consequence of this behavior is that when the exact absolute location of any one feature is provided to the fully correlated map, the exact absolute location of the vehicle or any other feature is deduced.

While single vehicle CML produces full correlations between the vehicle and the features (and thus zero relative error), the absolute error for the vehicle and each feature does not reduce to zero [29][30].

Theorem III.3: In the limit as the number of observations increases, the lower bound on the covariance matrix of the vehicle or any single feature is determined only by the initial vehicle covariance at the time of the observation of the first feature.

This theorem states that in the single vehicle CML case, the absolute error for the vehicle or single feature can never be lower than the absolute vehicle error present at the time the first feature is initialized into the SM filter.

IV. EXTENDING CML TO MULTIPLE VEHICLES

In the collaborative CML algorithm, all of the collaborating vehicle state estimates are combined into a single state vector $\mathbf{x_v}[k] = [\mathbf{x_v^A}[k]^T \mathbf{x_v^B}[k]^T \dots \mathbf{x_v^N}[k]]^T$, where $\mathbf{x_v^i}[k]$ is the vehicle state estimate for vehicle i at time k. As in single vehicle stochastic mapping, the feature state estimate of the jth point landmark in the environment at time step k is represented by the position estimate $\mathbf{x_{f_j}}[k]$, generating a com-

bined feature estimate for this environment of $\mathbf{x_f}[k] = [\mathbf{x_{f_1}}[k]^T \mathbf{x_{f_2}}[k]^T \ldots \mathbf{x_{f_n}}[k]^T]^T$. A single combined state estimate is then defned that incorporates all of the vehicle and feature estimates, defned as

$$
\mathbf{x}[k] = \left[\begin{array}{c} \mathbf{x_v}[k] \\ \mathbf{x_f}[k] \end{array} \right] = \left[\begin{array}{c} \mathbf{x_v^A}[k] \\ \mathbf{x_v^B}[k] \\ \vdots \\ \mathbf{x_v^N}[k] \\ \mathbf{x_{f_1}}[k] \\ \mathbf{x_{f_2}}[k] \\ \vdots \\ \mathbf{x_{f_n}}[k] \end{array} \right] . \quad (2)
$$

The associated covariance matrix $\mathbf{P}[k+1|k]$ is maintained which represents the £rst order uncertainty and correlations present in the $\mathbf{x}[k+1|k]$ state estimate. We use super-scripted letters to reference vehicles and numbers for super-scripted features. The general collaborative CML covariance matrix $\mathbf{P}$ can be written as

$$
\left[\begin{array}{cccccccc} \mathbf{P^{AA}} & \mathbf{P^{AB}} & \ldots & \mathbf{P^{AN}} & \mathbf{P^{A1}} & \mathbf{P^{A2}} & \ldots & \mathbf{P^{An}} \\ \mathbf{P^{BA}} & \mathbf{P^{BB}} & \ldots & \mathbf{P^{BN}} & \mathbf{P^{B1}} & \mathbf{P^{B2}} & \ldots & \mathbf{P^{Bn}} \\ \vdots & \vdots & \ddots & \vdots & \vdots & \vdots & \ldots & \vdots \\ \mathbf{P^{NA}} & \mathbf{P^{NB}} & \ldots & \mathbf{P^{NN}} & \mathbf{P^{N1}} & \mathbf{P^{N2}} & \ldots & \mathbf{P^{Nn}} \\ \mathbf{P^{1A}} & \mathbf{P^{1B}} & \ldots & \mathbf{P^{1N}} & \mathbf{P^{11}} & \mathbf{P^{12}} & \ldots & \mathbf{P^{1n}} \\ \mathbf{P^{2A}} & \mathbf{P^{2B}} & \ldots & \mathbf{P^{2N}} & \mathbf{P^{21}} & \mathbf{P^{22}} & \ldots & \mathbf{P^{2n}} \\ \vdots & \vdots & \vdots & \vdots & \vdots & \vdots & \ddots & \vdots \\ \mathbf{P^{nA}} & \mathbf{P^{nB}} & \ldots & \mathbf{P^{nN}} & \mathbf{P^{n1}} & \mathbf{P^{n2}} & \ldots & \mathbf{P^{nn}} \end{array} \right] .
$$
$$(3)$$

where for example $\mathbf{P^{B2}}$ is the cross correlation in estimates of the location of vehicle B and feature 2.

Once collaborating vehicles are added into the state and covariance vectors, the multi-vehicle SM prediction and update equations take on the same general form as the single vehicle SM algorithm. For a complete statement of the multi-vehicle SM prediction and update equations, see [28].

V. COLLABORATIVE CML PERFORMANCE ANALYSIS

This section presents the collaborative CML extension of single vehicle SM error convergence properties, and quanti£es the best-case performance of collaborative CML. These performance characteristics are validated via simulation in Section VI. The theorems derived and brie¤y reviewed in Section III serve the theoretical basis for analyzing the performance of the collaborative CML algorithm.

The full correlation property of single vehicle CML asserted in Theorem III.2 scales to the collaborative CML case, as the second vehicle is, in essence, a moving feature in the SM structure.

Theorem V.1: In the limit as the number of observations increases, if there are features observed by all vehicles, or each vehicle directly observes its collaborators, all of the vehicle and feature estimates become completely correlated with each other.

However, the single vehicle CML lower performance bound does not apply to the collaborative CML case. Multiple vehicles performing CML together can attain a lower absolute error than the single vehicle initial covariance which bounds the single vehicle CML case. The collaborative lower bound is quanti£ed in the following theorem:

Theorem V.2: In the collaborative CML case, in the limit as the number of observations increases, the lower bound on the covariance matrix of any vehicle or any single feature equal to the inverse of the sum the initial collaborating vehicle covariance inverses at the time of the observation of the £rst feature or observation of a collaborating vehicle.

Analysis of the limiting behavior of the state covariance matrix in the collaborative case is performed by applying the information form of the Kalman £lter [31]. The full proof is introduced in detail by [28], the intermediary result of which is

$$
\lim_{k \to \infty} \mathbf{P^{AA}}[k|k] = \lim_{k \to \infty} \mathbf{P^{BB}}[k|k]
$$
$$
= \mathbf{P^{AA}}[0]\mathbf{P^{BB}}[0]\left[\ \mathbf{P^{AA}}[0] + \mathbf{P^{BB}}[0] \ \right]^{-1} . \ (4)
$$

This result is the lower performance bound for collaborative CML with two vehicles. Note that the vehicle covariances for both vehicles become fully correlated and thus identical, supporting Theorem III.2. A simpler, more intuitive conceptual result is found by taking the inverse of Equation 4, producing a result of

$$
\lim_{k \to \infty} \mathbf{P^{AA^{-1}}}[k|k] = \lim_{k \to \infty} \mathbf{P^{BB^{-1}}}[k|k]
$$
$$
= \mathbf{P^{AA^{-1}}}[0] + \mathbf{P^{BB^{-1}}}[0] . \quad (5)
$$

Equation 5 makes sense in the context of conservation of information. In the general case, $\mathbf{P^{-1}}$ represents the amount of information present in the system [31]. The total amount of information in the system can never decrease, but can stay constant when no noise is added to the system. The sum of information present initially in the system is equal to the inverse of the sum of initial uncorrelated vehicle position errors, while the amount of information present after in£nite observations are made is encapsulated in a single vehicle position covariance.

It is also important to note that the lower performance bound for collaborative CML is not dependent on direct observation of one vehicle by another. While direct observation improves the rate of covariance convergence, simple observation by both vehicles of a common feature is all that is required for convergence.

Equation 5 scales easily for collaboration with more

than two vehicles. Assume that at time $t \approx \infty$ a third vehicle C, with a nonzero initial covariance uncorrelated with vehicle A and vehicle B, becomes a collaborator. Thus the lower performance bound becomes

$$\mathbf{P^{AA^{-1}}}[t] = \mathbf{P^{BB^{-1}}}[t] = \mathbf{P^{AA^{-1}}}[0] + \mathbf{P^{BB^{-1}}}[0] . \tag{6}$$

Since vehicles A and B are fully correlated at t, $\mathbf{P^{AA^{-1}}}[t]$ captures all of the information present in vehicle $\mathbf{P^{BB^{-1}}}[t]$. Thus

$$\lim_{k \to \infty} \mathbf{P^{AA^{-1}}}[k|k] = \lim_{k \to \infty} \mathbf{P^{BB^{-1}}}[k|k]$$
$$= \lim_{k \to \infty} \mathbf{P^{CC^{-1}}}[k|k]$$
$$= \mathbf{P^{AA^{-1}}}[\mathbf{t}] + \mathbf{P^{CC^{-1}}}[\mathbf{t}]$$
$$= \mathbf{P^{AA^{-1}}}[\mathbf{0}] + \mathbf{P^{BB^{-1}}}[\mathbf{0}] + \mathbf{P^{CC^{-1}}}[\mathbf{t}] . \tag{7}$$

In the n vehicle case, the lower performance bound becomes

$$\lim_{k \to \infty} \mathbf{P^{AA^{-1}}}[k|k] = \lim_{k \to \infty} \mathbf{P^{BB^{-1}}}[k|k]$$
$$= \cdots = \lim_{k \to \infty} \mathbf{P^{NN^{-1}}}[k|k]$$
$$= \mathbf{P^{AA^{-1}}}[i_\mathbf{A}] + \mathbf{P^{BB^{-1}}}[i_\mathbf{B}]$$
$$+ \cdots + \mathbf{P^{NN^{-1}}}[i_\mathbf{N}] , \tag{8}$$

where i_n represents the initial time at which the nth vehicle started collaborating, assuming that each vehicle covariance is initially uncorrelated with its collaborators. In the case of homogeneous collaborating vehicles, each with identical, initially uncorrelated error estimates, such that

$$\mathbf{P^{AA}}[\mathbf{0}] = \mathbf{P^{BB}}[\mathbf{0}] = \cdots = \mathbf{P^{NN}}[\mathbf{0}] , \tag{9}$$

a relationship can be found between the £nal map covariance and the number of vehicles required to achieve this performance bound, de£ned by,

$$\lim_{k \to \infty} \mathbf{P^{final^{-1}}}[k|k]$$
$$= \mathbf{P^{AA^{-1}}}[\mathbf{0}] + \mathbf{P^{BB^{-1}}}[\mathbf{0}] + \cdots + \mathbf{P^{NN^{-1}}}[\mathbf{0}] ,$$
$$= n\mathbf{P^{NN^{-1}}}[\mathbf{0}] . \tag{10}$$

Taking the determinant of both sides and solving for n produces a result of

$$n = \frac{det(\mathbf{P^{desired^{-1}}})}{det(\mathbf{P^{NN^{-1}}}[\mathbf{0}])} , \tag{11}$$

where $\mathbf{P^{desired}}$ is the desired £nal map error. This result is very useful for mission planning as it allows determination of how many vehicles are required to construct a map to a desired accuracy.
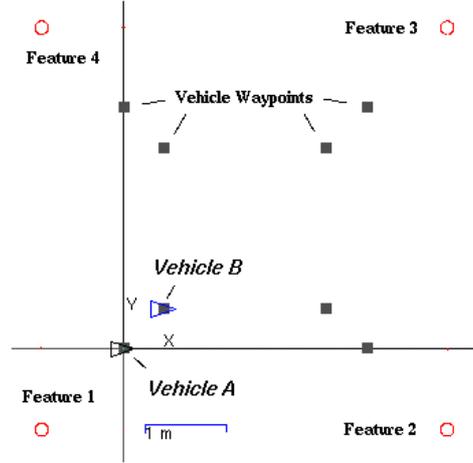

Fig. 1. Feature and initial vehicle positions

VI. COOPERATIVE CML IMPLEMENTATION

This section presents 2-D CML simulation results that demonstrate the quantitative CML performance gains from collaboration. The simulation uses two collaborating vehicles traveling in concentric squares, observing each other as well as four static point features in the environment. In the £rst of two simulation scenarios, the vehicles are given initial uncertainty and zero process noise, demonstrating convergence to the theoretical lower performance bound stated by Theorem V.2. The second scenario compares single vehicle and collaborative CML performance given both process noise and initial vehicle uncertainty. Table I summarizes the global parameters consistent for both scenarios. Initial vehicle locations, feature locations, and vehicle path waypoints are also kept consistent.

TABLE I
COLLABORATIVE CML SIMULATION GLOBAL PARAMETERS

number of vehicles	2
number of features	4
sampling period	0.2 sec.
simulation length	300 sec.
range measurement std. dev.	0.2 m
bearing measurement std. dev.	10 deg
vehicle cruise speed	0.5 m/s

A. Cooperative CML Scenario #1

In this scenario, there is no process noise added as each vehicle moves. However, each vehicle has an initial position uncertainty. Because of the zero additive process noise, dead reckoning error stays constant
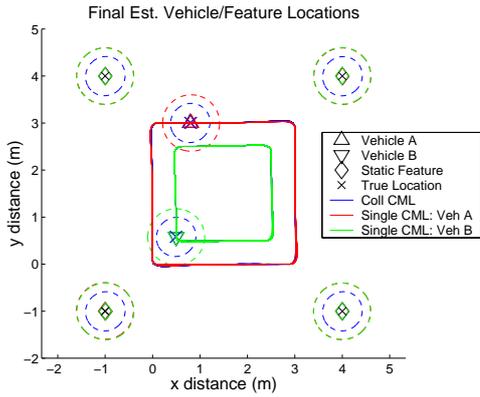
Fig. 2. CCML scenario #1 : position estimate comparison

x position process noise std. dev.	0.0 m/s
y position process noise std. dev.	0.0 m/s
heading process noise std. dev.	0.0 deg/s
velocity process noise std. dev.	0.0 m/s
initial vehicle x position uncertainty std. dev.	0.2 m
initial vehicle y position uncertainty std. dev.	0.2 m
initial heading position uncertainty std. dev.	0.0 deg

since no information is lost due to movement. The extra information provided by the initially uncorrelated position of the collaborating vehicle produces a reduction in position uncertainty as the collaborating vehicle is directly observed. Tables I and II summarize the parameters used for this scenario.

The initial starting location of both vehicles is shown by Figure 1. A direct comparison between vehicle and feature position errors at the end of the simulation is made in Figure 2, using 3σ error bound ellipses. Figure 3 shows plots of the position and heading errors of vehicle A versus time, along with 3σ bounds.

Vehicle A position error is presented in determinant form in Figure 4. Because of the zero additive process noise, position error never increases. However, the single vehicle CML error remains constant, supporting Theorem III.3, which states that position uncertainty for single vehicle CML can never be lower than the initial uncertainty. This plot also clearly shows the decrease in collaborative CML error uncertainty to the theoretical lower bound predicted by Equation 8. The extra information provided by the initially uncorrelated position of the collaborating vehicle provides a reduction in position uncertainty as information is shared. Note that the collaborative CML error determinant generated by this simulation is slightly less than that predicted. This slight overcon£dence can be attributed to the linearization process inherent in the EKF-based stochastic mapping algorithm. The performance of vehicle B is similar to vehicle A and thus vehicle B £gures are excluded for brevity.

Figure 5 plots the error estimate for Feature 1 in determinant form. This plot demonstrates the convergence of the feature estimate to the same uncertainty as the collaborating vehicles, supporting Theorem III.2. This plot is representative of the error performance of all four features.
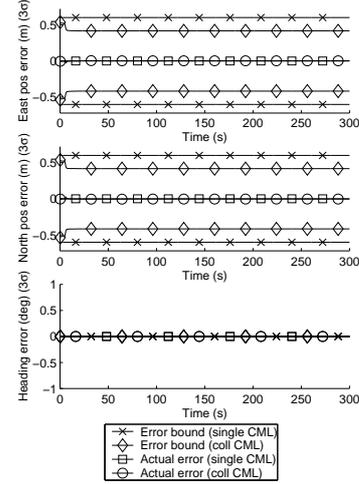

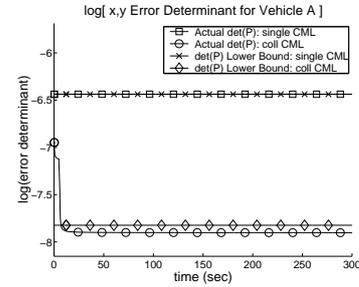Fig. 3. CCML scenario #1 : vehicle A error comparison

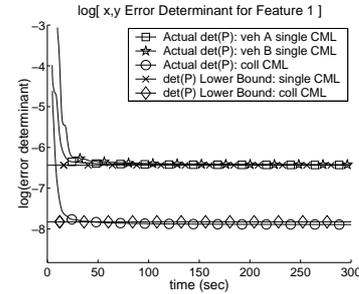Fig. 4. CCML scenario #1 : vehicle A error determinant

Fig. 5. CCML scenario #1 : feature 1 error determinant

B. Cooperative CML Scenario #2

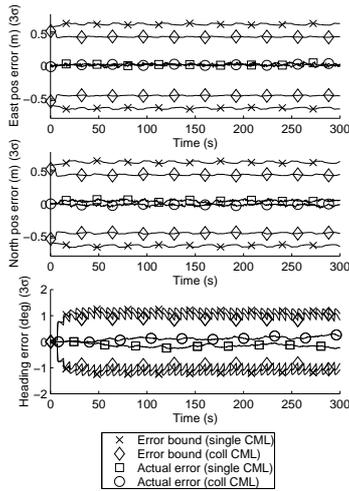This scenario best simulates an actual vehicle implementation, as both initial position uncertainty and

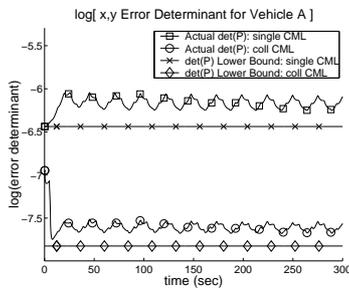Fig. 6. CCML scenario #2 : vehicle A error comparison

x position process noise std. dev.	0.2 m/s
y position process noise std. dev.	0.25 m/s
heading process noise std. dev.	0.2 deg/s
velocity process noise std. dev.	0.0 m/s
initial vehicle x position uncertainty std. dev.	0.075 m
initial vehicle y position uncertainty std. dev.	0.075 m
initial heading position uncertainty std. dev.	0.0 deg

Fig. 9. CCML scenario #2 : position estimate comparison

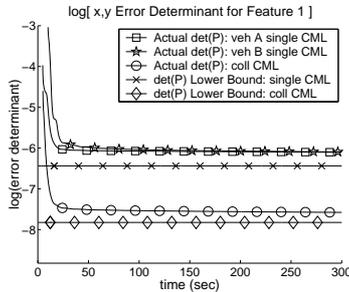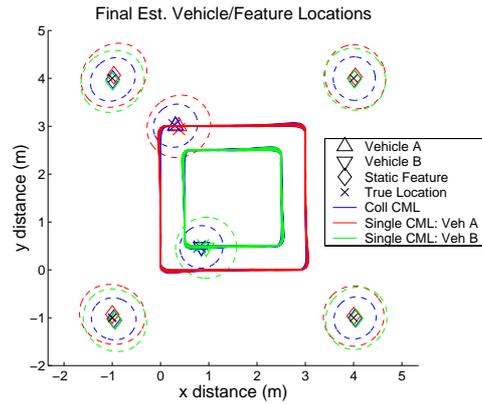Fig. 7. CCML scenario #2 : vehicle A error determinant

Fig. 8. CCML scenario #2 : feature 1 error determinant

process noise are present. Tables I and III summarize the parameters used for this scenario. As in the £rst scenario, Figures 9 and 8 show the error bound improvements made through collaboration. Figure 6 demonstrates that vehicle position uncertainty stabilizes above the theoretical lower performance bound in the presence of process noise.

C. Practical Implementation

The collaborative CML algorithm has been implemented using the system described in [32]. In the results described here and illustrated in £gure 10 two mo-

bile B21R robots ($B21a$ and $B21b$) equipped with a SICK laser scanner were tele-operated to move around an entrance hall of a building. $B21a$ started performing CML as it moved around the workspace. A minute or so later $B21b$ began operating, augmenting the map building processes. The initial uncertainty in $B21a$'s position was set to zero. That of $B21b$ however was set to tens of meters. The joint compatibility branch and bound (JCBB) data association algorithm [33] was used by both vehicles and facilitated the initialization of $B21b$ into the map being built by $B21a$. The initial large uncertainty of $B21b$ meant that the data association step implicitly localized the vehicle within the map already being built by the $B21a$. The JCBB algorithm places great weight on the *mutual* consistency of correspondences between sets of features and observations. Despite the presence of gross vehicle uncertainty the branch and bound search is able to discount mutually inconsistent observation/feature associations. The most probable correspondences deduced, the large initial uncertainty in $B21b$ admits a large change in its state estimate during the ensuing Kalman update stage. This represents the localization of $B21b$ into the map re£ning a crude initial guess. An alternative and more general approach would involve using JCBB to test not just hypothesized correspondences between observa-
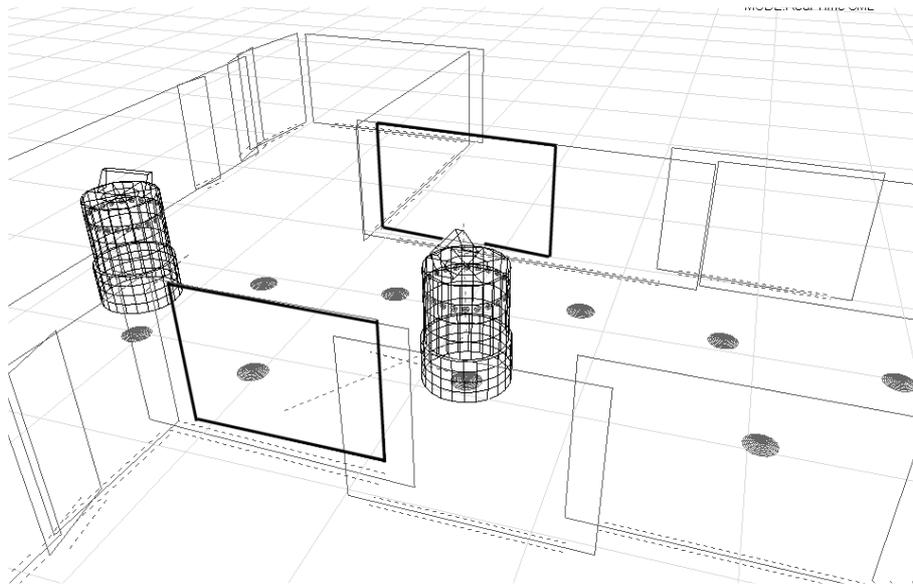
Fig. 10. A snapshot of the output of a realtime CCML implementation using two mobile B21R robots

tions and mapped features but also feature to feature correspondences using separate maps built by separate vehicles. This work is in progress.

VII. CONCLUSION

Current algorithms for this concurrent mapping and localization (CML) problem have been implemented for single vehicles, but do not account for extra positional information available when multiple vehicles operate simultaneously. This paper introduced an innovative technique for combining sensor readings for multiple autonomous vehicles, enabling them to perform cooperative CML. In addition, a lower algorithmic performance bound for collaboration has been determined, enabling calculation of the number of cooperating vehicles required to accomplish a given task. This quanti£es intuitive performance bene£ts that result from using more than one vehicle for mapping and navigation, which were validated in simulation.

Acknowledgments

REFERENCES

[1] R. Arkin and T. Balch, "Behavior-based formation control for multi-robot teams," *IEEE Transactions on Robotics and Automation*, vol. 14, no. 6, pp. 926–239, 1998.

[2] L. Parker, "Current state of the art in distributed autonomous mobile robotics," *Distributed Autonomous Robotic Systems 4*, vol. 4, pp. 3–12, 2000.

[3] D. Kortenkamp, R. P. Bonasso, and R. Murphy, Eds., *Arti£cial intelligence and mobile robots*, AAAI Press/MIT Press, Cambridge, MA, 1998.

[4] R. Vaughan, K. Stoy, G. Sukhatme, and M. Mataric, "Whistling in the dark: cooperative trail following in uncertain localization space," in *Proceedings of International Conference on Autonomous Agents*, Barcelona, Spain, 2000.

[5] W. Cohen, "Adaptive mapping and navigation by teams of simple robots," *Robotics and Autonomous Systems*, vol. 18, pp. 411–434, 1996.

[6] K. Sty, "Using situated communication in distributed autonomous mobile robots," in *Seventh Scandinavian Conference on Arti£cial Intelligence (SCAI01)*, 2001.

[7] J. Spletzer, A. Das, R. Fierro, C. Taylor, V. Kumar, and J. Ostrowski, "Cooperative localization and control for multi-robot manipulation," in *submitted to International Conference on Intelligent Robots and Systems*, Hawaii, Dec 2001, URL: http://www.cis.upenn.edu/mars/sdftko-iros01.pdf [cited 12 Apr 2001].

[8] D. Jung, J. Heinzmann, and A. Zelinsky, "Range and pose estimation for visual servoing on a mobile robotic target," in *Proceedings, IEEE International Conference on Robotics and Automation*, 1998.

[9] S. Roumeliotis and G. Bekey, "Synergetic localization for groups of mobile robots," in *Proceedings of IEEE Conference on Decision and Control*, Sydney, Australia, Dec 2000.

[10] S. Roumeliotis and G. Bekey, "Distributed multi-robot localization," in *Proceedings of the Fifth International Symposium on Distributed Autonomous Robotic Systems*, Knoxville, TN, 2000, pp. 241–250.

[11] H. Singh, J. Catipovic, R. Eastwood, L. Freitag, H. Henriksen, F. Hover, D. Yoerger, J. Bellingham, and B. Moran, "An integrated approach to multiple AUV communications, navigation, and docking," in *In IEEE Oceans*, 1987, pp. 59–64.

[12] D. Atwoood, J. Leonard, J. Bellingham, and B. Moran, "An acoustic navigation system for multiple vehicles," in *Proceedings, International Symposium on Unmanned Untethered Submersible Technology*, 1995, pp. 202–208.

[13] R. Vaughan, G. Sukhatme, J. Mesa-Martinez, and J. Montgomery, "Fly spy: lightweight localization and target tracking for cooperating ground and air robots," in *Proceedings of the Fifth International Symposium on Distributed Autonomous Robotic Systems*, 2000.

[14] M. Mataric, "Coordination and learning in multi-robot systems," *IEEE Intelligent Systems*, pp. 6–8, 1998.

[15] R. Brooks, "Intelligence without reason," *MIT AI Lab Memo 1293*, 1991.

[16] G. Dedeoglu and G. Sukhatme, "Landmark-based matching algorithm for cooperative mapping by autonomous robots," in *Proceedings of the Fifth International Symposium on Distributed Autonomous Robotic Systems*, 2000.

[17] A. Billard, A. Ijspeert, and A. Martinoli, "A multi-robot system for adaptive exploration of a fast changing environment: Probabilistic modelling and experimental study," *Connection Science*, vol. 11, no. 3/4, pp. 357–377, 2000.

[18] S. Thrun, "A probabilistic on-line mapping algorithm for teams of mobile robots," *International Journal of Robotics Research*, vol. 20, no. 5, pp. 335–363, May 2001.

[19] D. Fox, W. Burgard, H. Kruppa, and S. Thrun, "A probabilistic approach to collaborative multi-robot localization," *Autonomous Robots*, vol. 8, no. 3, pp. 325–344, June 2000.

[20] A. Doucet, N. de Freitas, and N. Gordan, Eds., *Sequential Monte Carlo Methods in Practice*, Springer-Verlag, 2001.

[21] J. Leonard and H. Feder, "Decoupled stochastic mapping," *MIT Marine Robotics Laboratory Technical Memorandum 99-1*, 1999.

[22] J. A. Castellanos and J. D. Tardos, *Mobile Robot Localization and Map Building: A Multisensor Fusion Approach*, Kluwer Academic Publishers, Boston, 2000.

[23] J. Guivant and E. Nebot, "Optimization of the simultaneous localization and map building algorithm for real time implementation," *IEEE Transactions on Robotic and Automation*, vol. 17, no. 3, pp. 242–257, June 2001.

[24] H. Choset and K. Nagatani, "Topological simultaneous localization and mapping (slam): toward exact localization without explicit localization," *IEEE Transactions on Robotic and Automation*, vol. 17, no. 2, pp. 125–137, April 2001.

[25] B. J. Kuipers, "The spatial semantic hierarchy," *Arti£cial Intelligence*, 2000.

[26] R. Smith, M. Self, and P. Cheeseman, "Estimating uncertain spatial relationships in robotics," *Autonomous Robot Vehicles*, pp. 167–193, 1990.

[27] H. Feder, *Simultaneous stochastic mapping and localization*, Ph.D. thesis, MIT Dept. of Mechanical Engineering, 1999.

[28] J. Fenwick, *Collaborative Concurrent Mapping and Localization*, S. M. thesis, MIT Dept. of Electrical Engineering and Computer Science, May 2001, http://deslab.mit.edu/~jfenwick/Public/.

[29] P. Newman, *On the structure and solution of the simultaneous localization and mapping problem*, Ph.D. thesis, University of Sydney, March 1999.

[30] M. W. M. G. Dissanayake, P. Newman, H. F. Durrant-Whyte, S. Clark, and M. Csorba, "A solution to the simultaneous localization and map building (slam) problem," *IEEE Transactions on Robotic and Automation*, vol. 17, no. 3, pp. 229–241, June 2001.

[31] P. Maybeck, *Stochastic models, estimation and control*, vol. 1, Academic Press, New York, 1979.

[32] P. Newman, J.Leonard, J.D. Tardós, and J.Neira, "Explore and return: Experimental validation of real time concurrent mapping and localization," in *Proc. IEEE Int. Conf. Robotics and Automation*. IEEE, 2002, p. TBA.

[33] J. Neira and J.D. Tardós, "Data association in stochastic mapping using the joint compatibility test," *IEEE Trans. on Robotics and Automation*, vol. 17, no. 6, pp. 890–897, 2001.